Development of a nanocapsule-loaded hydrogel for drug delivery for intraperitoneal administration

Bhanu Teja Surikutchi [a,c], Rebeca Obenza-Otero [c], Emanuele Russo [c], Mischa Zelzer [c], Irene Golán Cancela [b], José A. Costoya [b], José Crecente Campo [a], Maria José Alonso [a,*], Maria Marlow [c,*]

[a] *Centre for Research in Molecular Medicine and Chronic Diseases (CIMUS), Campus Vida, Universidade Santiago de Compostela, Santiago de Compostela 15706, Spain*
[b] *Molecular Oncology Laboratory MOL, Departamento de Fisioloxía, Centre for Research in Molecular Medicine and Chronic Diseases (CIMUS), Facultade de Medicina, Campus Vida, Universidade de Santiago de Compostela, Instituto de Investigación Sanitaria de Santiago de Compostela (IDIS), Santiago de Compostela 15706 Spain*
[c] *School of Pharmacy, University of Nottingham, University Park Campus, Nottingham NG7 2RD, United Kingdom*

ABSTRACT

Intraperitoneal (IP) drug delivery of chemotherapeutic agents, administered through hyperthermal intraperitoneal chemotherapy (HIPEC) and pressurized intraperitoneal aerosolized chemotherapy (PIPAC), is effective for the treatment of peritoneal malignancies. However, these therapeutic interventions are cumbersome in terms of surgical practice and are often associated with the formation of peritoneal adhesions, due to the catheters inserted into the peritoneal cavity during these procedures. Hence, there is a need for the development of drug delivery systems that can be administered into the peritoneal cavity. In this study, we have developed a nanocapsule (NCs)-loaded hydrogel for drug delivery in the peritoneal cavity. The hydrogel has been developed using poly(ethylene glycol) (PEG) and thiol-maleimide chemistry. NCs-loaded hydrogels were characterized by rheology and their resistance to dilution and drug release were determined *in vitro*. Using IVIS® to measure individual organ and recovered gel fluorescence intensity, an *in vivo* imaging study was performed and demonstrated that NCs incorporated in the PEG gel were retained in the IP cavity for 24 h after IP administration. NCs-loaded PEG gels could find potential applications as biodegradable, drug delivery systems that could be implanted in the IP cavity, for example at a the tumour resection site to prevent recurrence of microscopic tumours.

1. Introduction

Malignancies and peritoneal adhesions are two major indications where intraperitoneal (IP) drug delivery is used (Bajaj and Yeo, 2010). In this work, we aimed at designing and developing a new drug delivery system for IP administration that could overcome issues associated with NC retention and solubility of drugs in existing systems for the treatment of malignancies associated with abdominal and pelvic organs. In fact, peritoneal malignancies are one of the leading forms of cancer, accounting for about 8–9 % of cancer deaths (Siegel et al., 2014). These primary cancers, which are associated with any of the peritoneal organs, are highly aggressive and exhibit metastasis within the peritoneal cavity and other peritoneal organs (Ceelen and Flessner, 2010; Siegel and Jemal, 2015). The standard of care for the treatment of these peritoneal malignancies is cytoreductive surgery of the macroscopic tumour mass

(Group, 2002). Intravenous (IV) chemotherapy is also given perioperatively or postoperatively to treat unresectable microscopic tumour residues to avoid recurrence (Bijelic et al., 2007; Glehen et al., 2004; Sugarbaker, 1998). These conventional IV chemotherapies are non-specific and pose severe side effects, compromising the quality of life of patients (Armstrong et al., 2006). Moreover, chemotherapeutic molecules need to cross the interface between blood capillaries and peritoneal membrane after systemic administration, in order to diffuse into the peritoneal fluid and reach the IP cavity. Hence, achieving effective IP local drug concentrations through IV therapy is a significant challenge (Flessner, 2005; Van der Speeten et al., 2009).

IP administration of chemotherapeutic drugs surpasses the blood-peritoneal membrane diffusion barrier and overcomes these challenges, offering a pharmacokinetic advantage in comparison to the IV route (Dedrick et al., 1978; Shimada et al., 2005). Hence, direct

administration of chemotherapeutic agents into the peritoneal cavity has been evaluated as an alternative therapeutic option to the IV route. However, IP delivery has many challenges associated with it. Current IP administration approaches involve the installation of catheters into the IP cavity through hyperthermal intraperitoneal chemotherapy (HIPEC) and pressurized intraperitoneal aerosolized chemotherapy (PIPAC), which can cause complications such as infections, catheter leakage, bowel distention pain and bowel perforations (Armstrong et al., 2006; Hasovits and Clarke, 2012; Walker et al., 2006). Another challenge associated with IP delivery is the rapid clearance of molecules from the cavity, leading to reduced therapeutic benefits due to poor coverage of the serosal surface during irrigation and poor tissue penetration (Dedrick and Flessner, 1997). This limitation can be attributed to the dynamic nature of the peritoneal cavity. Peritoneal fluid fills the peritoneal cavity, providing an aqueous environment rich in proteins and electrolytes, to bathe the peritoneal organs. Under cancerous conditions, osmotic pressure builds up in the abdominal cavity, due to high protein content as a result of leaky blood vessels associated with the tumour, raising the total peritoneal fluid volume and increasing the fluid turnover. This fluid is called ascites fluid, which is a common manifestation in patients with peritoneal malignancies (Feldman et al., 1972; Senger et al., 1983). In order to attain desired therapeutic outcomes, chemotherapeutic agents must be retained in this dynamic environment. Hence, the development of drug delivery systems with retention in the peritoneal cavity would be advantageous not only to achieve desired pharmacokinetic and pharmacodynamic benefits but also to reduce the complications associated with IP administered catheters.

Drug delivery systems, including nanoparticles (NPs) (Amoozgar et al., 2014; Yang et al., 2013), nanocrystals (De Smet et al., 2012), liposomes (Sadzuka et al., 2000), microspheres (Kohane et al., 2006), and hydrogels (Li et al., 2012) have been explored as a way to enhance the retention of drugs in the peritoneal cavity. Among particulate drug delivery systems, both micro and NPs have some advantages and disadvantages. By virtue of their size, microparticles tend to be retained in the peritoneal cavity (Kohane et al., 2006). However, microparticles might cause potential risks of peritoneal adhesions and local inflammation (Kohane and Langer, 2010; Kohane et al., 2006). In contrast, NPs do not cause peritoneal adhesions, although they tend to be cleared from the cavity relatively fast. In addition, NPs are able to cross cell membranes by endocytosis, enhancing intracellular drug delivery (Ernsting et al., 2013; Huo et al., 2013; Simón-Gracia et al., 2016).

To overcome the rapid clearance of NPs from the IP cavity, a composite system can be designed to entrap the NPs in a hydrogel (Dakwar et al., 2017). An efficient composite can control the release of NPs and thereby retain them longer in the IP cavity. The rate of release of NPs into the cavity depends on the degradation of the hydrogel. Thermosensitive hydrogels that can flow freely at low temperatures and are able to gel at body temperature and under physiological conditions, have been explored for this purpose (Chen et al., 2018; Fan et al., 2015; Xu et al., 2016). In these hydrogels, gelation occurs by physical interactions between polymeric chains due to temperature changes upon injection. However, due to their weak physical interactions, thermosensitive hydrogels tend to be less resistant to dilution and high fluid turnover rates of the IP cavity, limiting their applicability in a clinical setting. In contrast, covalently cross-linked hydrogels are less susceptible to dilution as the degradation mechanism involves breakage of covalent bonds, instead of mere weakening of physical interactions (Nguyen and Lee, 2010; Pereira and Bártolo, 2014). This phenomenon could be beneficial in fluid rich environments such as the IP cavity. For instance, covalently cross-linked hyaluronic acid (HA) hydrogels reported by Bajaj G et al. were found to remain for up to 14 days in the IP cavity (Bajaj et al., 2012). In contrast, a non-chemically cross-linked, thermosensitive hydrogel prepared using a triblock copolymer, poly(ethylene glycol)-poly(caprolactone)-poly(ethylene glycol) (PEG-PCL-PEG), containing 5-fluorouracil, required repeated dosing over the same time period to achieve therapeutic efficacy (Wang et al., 2010). Thus, chemically cross-

linked hydrogels have the potential to further increase drug retention in the IP cavity.

However, longer retention does not necessarily ensure beneficial therapeutic outcomes. The therapeutic efficacy of a composite drug delivery system depends on a complex range of factors, which include rate of hydrogel degradation, rate of release of the active and effective penetration into the tumour mass. The covalently cross-linked HA hydrogel developed by Bajaj G et al. incorporated paclitaxel particles in the micrometre size range (Bajaj et al., 2012). These particles have to undergo dissolution to show a therapeutic effect, which is limited in case of hydrophobic molecules. In contrast, incorporating these hydrophobic molecules in a solution state in a nanoparticulate system would overcome the limitation of slow dissolution, while providing the size-related benefits of NPs. Thus, the use of a NP-hydrogel composite as a delivery system could be ideally placed for IP delivery, simultaneously extending IP residence time of the drug-loaded NPs.

Our laboratory has pioneered the development of NCs that are composed of an oily core, which enables the encapsulation of hydrophobic drugs, surrounded by a hydrophilic polymer shell (Fernandez et al., 2016). Ampuero et al. pioneered the development of HA NCs through a solvent displacement technique, consisting of a lipid core and HA shell, for intracellular delivery of hydrophobic anticancer drugs. These NCs not only showed storage stability upon freeze drying but also significant enhancement of cytotoxicity of DCX in an in vitro cancer cell line (Oyarzun-Ampuero et al., 2013). We have also previously developed a fibrin-based hydrogel system containing HA nanocapsules intended for the intra-articular delivery of anti-inflammatory drugs (Storozhylova et al., 2020). The objective of the current study was the development and characterization of a NC/gel-based composite drug delivery system that displays retention of the NCs in the peritoneal cavity. To achieve this, we developed a chemically cross-linked PEG-based hydrogel containing drug-loaded HA NCs. In a first step, we developed the HA NCs through a self-emulsification method in contrast to solvent displacement, which would render higher drug loading. Different surfactants, oils and HA of various molecular weights were explored to understand their influence on the physicochemical properties of the NCs. Finally, a covalently cross-linked PEG hydrogel was developed using a thiol-maleimide reaction. The novelty of this study is the incorporation of NCs into a covalently cross-linked PEG gel for IP drug delivery. Furthermore, this composite was characterized with rheology, and for in vitro drug release and then in vivo biodistribution using fluorescence imaging was measured. In addition, a physically cross-linked hydrogel loaded with DCNC, prepared from fibrin-hyaluronic acid (Fn-HA), was used to develop the in vivo fluorescence imaging (IVIS® protocols). This gel was used for the fluorescence imaging development as it was well established in our laboratory (Storozhylova et al., 2020).

2. Materials and methods

2.1. Materials

Fibrinogen and thrombin, both from human blood plasma were purchased from Sigma-Aldrich, Spain. Different molecular weights (M_n) of HA (research grade), 41–65 kDa, 500–749 kDa and 1.01–1.8 MDa, were purchased from Lifecore, USA. Tween® 80, good manufacturing practice (GMP) grade, was purchased from Acofarma, Spain. Lipocol® HCO-40 was obtained from Lipo Chemicals, USA. Labrasol and Labrafac™ Lipophile WL1349 (EP and USP compliant grades) were procured from Gattefossé, France. Benzethonium chloride (BZT) was purchased from Spectrum, USA. DXM (99.7% purity) was purchased from Acofarma, Spain. DCX (98% purity) was purchased from Acros Organics, Thermo Fisher Scientific, UK. PEG (M_n 3350) and fluorescent label, 1,1″-dioctadecyl-3,3,3″,3″-tetramethylindotricarbocyanine iodide (DiR) was purchased from Thermo Fisher Scientific, UK. 4-arm PEG maleimide (PEG-MAL, M_n 10 kDa) was purchased from Advanced BioChemicals,

LLC, USA, while *p*-toluenesulfonic acid, dithiothreitol (DTT), 3-mercaptopropionic acid, HEPES, Bovine serum albumin (BSA) (≥98%), sodium chloride (NaCl), sodium azide (NaN$_3$), calcium chloride dihydrate (CaCl$_2$·2H$_2$O), potassium chloride (KCl), magnesium chloride (MgCl$_2$), sodium phosphate dibasic (Na$_2$HPO$_4$), potassium phosphate monobasic (KH$_2$PO$_4$) was purchased from Sigma-Aldrich®, UK. Phosphate buffer saline (PBS, 0.01 M) tablets were also procured from Sigma-Aldrich®, UK. 1 M Tris buffer (pH 8.0) was purchased from Thermo Fisher Scientific, UK. All organic solvents used were HPLC grade. In-house ultrapure (Milli-Q) or endotoxin-free water was used throughout the experiments. Laboratory glassware was previously sterilized in an autoclave (Systec, Germany) prior to *in vivo* experiments and preparation carried out in a laminar flow unit.

2.2. Development and optimization of HA NCs

2.2.1. Optimization of NCs

NCs were developed using a self-emulsification technique by screening various oils and surfactants to form a nanoemulsion. Olive oil, Labrafac^{TM} Lipophile WL 1349 (from now-onwards it is written as Labrafac) and castor oil were used as the oils, while Kolliphor® RH 40, Labrasol and Tween® 80 were used as surfactants. Initially, physical mixtures of surfactant at 20% w/w and oil at 30% w/w were prepared in water and physical stability was evaluated by observing the phase separation after leaving the mixtures at 25 ± 5 °C for 24 h. The combinations that were stable, as observed visually and under the optical microscope (Zeiss International, Germany), were selected for further screening. DXM, a model hydrophobic molecule was incorporated into these mixtures at a concentration of 2, 6 and 8 mg/mL, to evaluate relative solubility and recrystallization. Ethanol, at a concentration of 13% w/w, was used as a cosolvent to dissolve DXM. Mixtures which showed solubility of DXM, but did not show recrystallization after leaving at 25 ± 5 °C for 24 h, were chosen for further evaluation. Identified mixtures were then optimized by varying the concentrations of surfactant (Tween® 80) from 15 to 30% w/w, a co-surfactant (Kolliphor® RH 40) from 10 to 15% w/w and oil (Labrafac) from 10 to 40% w/w. These mixtures were then left at 25 ± 5 °C for 3 days and physical stability was observed visually and using an optical microscope (Zeiss International, Germany). The combination of oils, surfactant and co-surfactant which gave a physical stable nanoemulsion in water, without inducing recrystallization of DXM was progressed as the basis for creating the NCs. NCs were manufactured by adding HA through electrostatic deposition onto a positively charged nanoemulsion manufactured by the addition of cationic BZT (0.1% w/w). The molecular weight and concentration of HA was optimized to obtain stable NCs with a low polydispersity index (PDI). HA with an average molecular weight of 40 kDa was evaluated at 0.1, 0.25 and 0.5% w/w concentrations, while HA with an average molecular weight of 700 kDa was evaluated at 0.1% w/w concentration to form NCs. Appropriate concentration and molecular weight were identified by evaluating the colloidal stability of NCs by measuring the particle size over a period of 28 days and entrapment efficiency of DXM over a period of 2 weeks at 2 – 8 °C (Method S1).

2.2.2. Preparation of blank NCs

For a 3 g batch size, 600 mg of Tween® 80, 300 mg of Labrafac and 300 mg of Kolliphor® RH 40 were mixed together to form an oil-surfactant mixture. 3 mg of BZT was dissolved separately in 500 μL of ethanol and this solution was added to oil-surfactant mixture to assist solubilization and impart positive charge to the nanoemulsions. A volume of 1050 μL of water was then injected into this composition, under stirring at 1500 rpm, using a syringe with 23 G needle. This process led to formation of a cationic nanoemulsion. 7.5 mg of HA (40 kDa) was separately dissolved in 330 μL of water (23 mg/mL) and this was added to the nanoemulsion using a syringe with 23 G needle, allowing the formation of a polymeric coating through electrostatic interaction, to

form NCs. NCs were isolated from free drug by centrifugation at 18,000 × g for 1 h at 15 °C. The cream layer, containing the nanocapsules, was then removed using a needle and syringe and then diluted with water up to a total weight of 3 g.

2.2.3. DiR loading

DiR was incorporated into NCs (DiNC) with a slight modification of the method described above. A working standard, 1000 ppm of DiR was prepared by diluting the stock solution (2.5 mg/mL of DiR in ethanol) with ethanol. To prepare DiNC, Tween® 80, Labrafac and Kolliphor® RH 40 were first weighed in an empty glass vial and mixed to form an oil-surfactant mixture. A solution of BZT in ethanol was then prepared and added to this mixture to attain a final concentration of 1 mg/mL BZT. DiR stock solution was then added and mixed well to obtain a final DiR concentration of 180, 120, 90 or 18 ppm DiNC, as required. NCs were then prepared by forming a nanoemulsion and electrostatic deposition of HA as described above.

2.2.4. DCX loading

The initial NC optimisation was carried out with DXM as a drug appropriate for peritoneal delivery. However DCX NCs were chosen to be incorporated in the PEG gel based on discussions with clinicians who identified that there was greater unmet clinical need for chemotherapeutic delivery. To obtain these DCX-loaded NCs (DCNC), a stock solution of DCX in ethanol (100 mg/mL) was first prepared. This was then added to the mixture of Tween® 80, Labrafac, Kolliphor® RH 40 and the ethanolic solution of BZT. After thorough mixing for 5 min, purified water was added to form a nanoemulsion. Further steps to prepare DCNC were the same as described earlier. Optimum DCX loading was identified by preparing DCNC at DCX final concentrations of 3, 7.5 and 12 mg/mL, followed by microscopic evaluation of DCNC for any traces of recrystallization.

2.3. Characterization of HA NCs

2.3.1. Particle size and zeta potential

The mean hydrodynamic diameter (size) and polydispersity index (PDI) of the NCs, DiNC and DCNC were measured after dilution (50 ×) with ultrapure water by dynamic light scattering (DLS) at 25 °C with an angle of detection at 173°. The zeta potential was measured by laser Doppler anemometry (LDA) using the same dilution in water. Both DLS and LDA analyses were performed using a Zetasizer®, NanoZS, Malvern Instruments, Malvern, UK.

2.3.2. Determination of DiR loading in NCs

The encapsulation efficiency (% EE) of DiR was determined after the isolation of DiNC by centrifugation at 18,000 × *g* for 1 h at 15 °C (Hettich, Universal 32R, Germany). A calibration curve of DiR in ethanol was prepared and fluorescence intensity was measured using a microplate reader (Tecan Infinite® 200 plate reader) at excitation and emission wavelengths of 745 and 795 nm respectively. The amount of DiR in the creamed layer (isolated DiNC), residual liquid beneath the creamed layer and the non-isolated (before centrifugation) DiNC were quantified by measuring the amount of fluorescence obtained from each fraction after approximately 50x dilution in ethanol to disrupt the NCs. The exact amount of dilution was calculated by weighing the sample before dilution. Equation 1 was used to determine % EE.

$$\% \; EE \; = \; \frac{Amount \; of \; DiR \; in \; isolated \; DiNC}{Total \; DIR \; added} \; \times \; 100$$

2.3.3. Encapsulation efficiency of DCNC

The amount of DCX in the supernatant (isolated DCNC), liquid underneath and the non-isolated (before centrifugation) DCNC were quantified by HPLC after extraction of DCX from respective samples. To extract DCX, a pre-weighed quantity (approx. 20 mg) of the sample was

diluted to 1 mL with ethanol, followed by vortex mixing for 3 min. The HPLC consisted of an Agilent system equipped with a UV detector set at 227 nm and a reverse phase Zorbax, Eclipse XDB- C8 column (4.6 ID × 150 mm, pore size 5 μm), Agilent, UK. The mobile phase was a mixture of ultrapure water and acetonitrile, each containing 0.1 %v/v ortho-phosphoric acid (55:45), isocratic, with a flow rate of 1 mL/min. The column was set at 25 °C and the injection volume was 20 μL. The standard calibration curve of DCX was linear in the range of 1–1000 μg/mL ($r^2 = 0.999$). The concentration of DCX obtained from these samples was used to calculate the encapsulation efficiency (% EE) and drug loading using equations 2 and 3 respectively.

$$\% \ EE \ = \ \frac{Amount \ of \ DCX \ in \ isolated \ \ DCNC}{Total \ DCX \ added} \times 100$$

$$\% \ Drug \ loading \ = \ \frac{Amount \ of \ DCX \ in \ isolated \ DCNC}{Amount \ of \ DCNC \ (mg)}$$

2.4. Preparation of NCs loaded in a Fn-HA hydrogel

The Fn-HA gel was prepared as described by Storozhylova *et al.*, using thrombin mediated enzymatic polymerization, where stock solutions of fibrinogen, thrombin and HAs were first prepared (Storozhylova et al., 2020). A lyophilized powder of human blood derived fibrinogen was dissolved in 0.15 M solution of NaCl at 37 °C to give a concentration of 25 mg/mL. The stock of solution of thrombin was prepared by dissolving lyophilized powder of human blood derived thrombin in 0.01 M phosphate buffer saline (PBS) to a concentration of 100 NIH-U/mL. BSA was added as a stabilizer to an equivalent final concentration of 1% w/w. Both the stock solutions of fibrinogen and thrombin were stored at −20 ± 2 °C. Before each experiment, an aliquot was thawed to 37 °C for not>2 h before the gel preparation. Later, stock solutions of HAs (700 kDa and 1.5 MDa MW), were prepared by separately dissolving these polymers in HEPES buffer (0.02 M HEPES, 0.1 M NaCl, 10^{-4} M CaCl$_2$, pH 7.4) to obtain individual concentrations of 0.65% w/v. A 1:1 mixture of these HA solutions was prepared before the gel preparation. NCs were incorporated at a concentration of 30 % w/w to obtain a NC-Fn gel. Later, DiNC and DCNC were incorporated into the Fn-HA gel, which are labelled as DiNC-Fn and DCNC-Fn respectively. Table S5 in ESI shows the composition of the Fn-HA gel.

2.5. Development of covalently crosslinked PEG hydrogels

Covalently crosslinked PEG gels were synthesized by crosslinking 4 armed PEG-MAL polymers with a linear PEG dithiol cross-linker (PEG-SH).

2.5.1. Synthesis of PEG dithiol crosslinker

Poly(ethylene glycol) (M$_n$ 3350) with two terminal hydroxyls was functionalised with thiols similarly to previously described (Nie et al., 2007). Equivalents (eq) were calculated with respect to hydroxyl group concentration. PEG (1 g, 0.6 mmol hydroxyl groups, 1 eq.), 3-mercapto-propionic acid (530 μL, 6 mmol, 10 eq.), *p*-toluenesulfonic acid (11.4 mg, 0.1 mmol, 0.1 eq.) and DTT (23 mg, 0.15 mmol, 0.5 eq.) were dissolved in toluene (20 mL) under nitrogen flow. The reaction was heated to reflux and left stirring under nitrogen atmosphere for 24 h. Toluene was then evaporated under vacuum and the polymer was precipitated thrice in cold acetone, which was kept at –20 °C for at least 15 min. The precipitated product was then dried, under vacuum at room temperature for 2 days. PEG-SH functionalisation was confirmed by ^{1}H NMR using a Bruker 400 Ultrashield.

^{1}H NMR (400 MHz, D$_2$O, δ, ppm): 4.35–4.30 (m, 4H, CH$_2$-O-C(O)), 3.94–3.48 (340H, (CH$_2$-CH$_2$-O)$_n$ from PEG backbone), 2.84–2.73 (m, 8H, CH$_2$-CH$_2$-SH) (Figure S3 in ESI).

2.5.2. Preparation of PEG gels

PEG-MAL and Thiol gels (from now onwards simplified as PEG gels) were prepared by Michael addition reaction between four-arm PEG-MAL and the synthesised PEG-SH crosslinker (Figure S4 in ESI). As the Michael addition is slower and therefore more controlled at lower pH, colloidal stability of NCs at low pH was screened to identify a suitable acidic environment that ensures controlled cross-linking while maintaining NCs stability. NCs were suspended in various low pH buffers (0.1 M citrate buffer pH 3 – 5), followed by the determination of particle size and PDI. 0.1 M pH 5.0 citrate was selected for hydrogel preparation as it has ensured colloidal stability of NCs.

Hydrogels were formed upon physical mixing aqueous solutions of PEG-MAL and PEG-SH in buffer (0.1 M pH 5.0 citrate). NC-PEG gels were prepared at 5 and 10 % w/w concentrations of PEG-MAL and a 1:1 thiol: maleimide molar ratio. PEG-MAL and PEG-SH were separately dissolved in the buffer. A suspension of NCs was then diluted in the buffer and added to the PEG-SH solution. The mixture of NCs and PEG-SH solution was added into the injection mould and PEG-MAL solution was added to it. The whole mixture (50 μL) was then mixed through 3–4 syringe piston strokes and left undisturbed at room temperature for at least 2 h to form the hydrogel. Table S4 in the ESI shows the composition of PEG gels at 5 and 10% w/w concentrations of PEG-MAL. NC-PEG gels have been incorporated with DiR and DCX to obtain DiNC loaded (DiNC-PEG) and DCNC loaded (DCNC-PEG) hydrogels respectively.

2.6. Characterization of NCs loaded hydrogels

2.6.1. Rheology

Modular compact rheometer (MCR302, Anton Paar GMBH, Austria) was used to perform dynamic rheology measurements for both NC-Fn and NC-PEG gels, with a 25 mm diameter rotating shaft. Oscillatory amplitude sweep studies were performed on NC-Fn gel using a parallel plate assembly (25 mm diameter). Approximately, 300 μL of gel components were placed on the center of the fixed plate. NC-Fn gel samples were prepared by combining mixtures of fibrinogen, NCs and HAs solutions to form a premix. Later, this premix was loaded into the syringe and thrombin was then taken into the loaded syringe. Mixing of components was performed by moving the plunger of the syringe six to seven times. This mixture was then extruded out of the syringe within 2 min onto the plate to avoid gel formation inside the syringe barrel. Gel samples were then allowed to set for 5 min over the plate without any intervention. After 5 min, the rotating shaft was allowed to come in contact with the gel. Then, oscillatory amplitude sweeps were performed in the strain range of 0.1% to 100% at a constant frequency of 10 rad s^{-1}, 25 °C and 0.5 mm gap between the parallel plates. Storage modulus (G') and loss modulus (G'') were recorded.

Similar to NC-Fn gel, a parallel plate assembly at 25 °C on the modular compact rheometer was used for NC-PEG gel. However, gelation kinetics were determined instead of oscillatory amplitude sweeps, by monitoring the increase of storage modulus (G') and loss modulus (G'') with time at a fixed 0.5 mm gap, 20 rad s^{-1} frequency and 0.5 % strain. NC-PEG gels prepared at 10% w/w PEG-MAL concentration were used for the study. 21.78 mg of PEG-SH and 90 mg of NCs that corresponds to 300 μL of NC-PEG gel, was added to 120 μL of citrate buffer (0.1 M, pH 5.0) to form a mixture of PEG-SH and NCs. A solution of PEG-MAL was then prepared by dissolving 30 mg of PEG-MAL in 90 μL of citrate buffer (0.1 M, pH 5.0) corresponding to 300 μL of PEG-MAL hydrogel. The viscoelastic properties were recorded after the addition of the mixture of PEG-SH and NCs to the bottom plate of the rheometer. It was then programmed to record the G' and G'' every 15 s, until 1800 s. The solution of PEG-MAL in citrate buffer was added after 60 s from the start of experiment. The gelation time was considered to be the crossover point of G' and G'', and the maximum G' achieved during the study was used to compare the mechanical properties.

2.6.2. Resistance to dilution

The ability of NC-Fn and NC-PEG gels to withstand the dilution was observed by incubating it in simulated intraperitoneal fluid (SIPF) at 37 °C. The composition of SIPF used for the study was obtained from literature, which consisted of BSA (3% w/v), NaCl (0.7% w/v), KCl (0.02% w/v), $CaCl_2$ (0.014% w/v), $MgCl_2$ (0.005% w/v), Sodium azide (0.05% w/v), Na_2HPO_4 (0.144% w/v) and KH_2PO_4 (0.024% w/v) (El-Kamel et al., 2019). DiNC-Fn gel was prepared as described previously, whereas DiNC-PEG gels were prepared at 5% and 10% w/w PEG-MAL concentrations. Three dilutions were considered at gel: SIPF ratios of 1:3, 1:9 and 1:25. The integrity of the gels after incubation was evaluated by visual observation.

2.6.3. In vitro release studies

In vitro release of DiR from DiNC-Fn and DiNC-PEG gels (both 5% and 10% PEG-MAL concentrations) was determined by incubating the DiNC loaded gels with SIPF at 37 °C. Gels were incubated at maximum tolerated dilution corresponding to each gel. DiNC-Fn gel was prepared, incorporating DiNC. 100 µL of the gel was incubated with 300 µL (1:3 dilution). At each time point, 50 µL of sample was collected and diluted with ethanol accordingly. Three repeat samples were taken at each time point. 50 µL of DiNC-PEG gel was prepared by incorporating DiNC. Gels were incubated with 1.25 mL of SIPF, yielding a 1:25 dilution at 37 °C. At each time point, 50 µL samples were collected and diluted with ethanol accordingly. Three repeat samples were undertaken at each time point. Fluorescence intensities of samples collected from both gels was recorded with the same procedure as used to determine DiR loading in the NCs.

In vitro release for DCX was also determined for PEG gels containing DCNC, by incubating the hydrogel with SIPF containing 0.5 % w/v Tween® 80 at 37 °C. Being a hydrophobic molecule, poor aqueous solubility of DCX might be a rate-limiting step to drug release into the medium. Hence, Tween® 80 was added to the medium to maintain sink conditions. 50 µL of DCNC-PEG gel was placed in a glass vial and 1.25 mL of media was added to achieve 1:25 dilution. At each time point, the whole volume of media was collected and replaced with fresh media. DCX was then extracted from these samples by evaporating the water from 1 mL of the sample using a nitrogen evaporator, followed by addition of 1 mL of ethanol to dissolve the DCX. This ethanolic solution was then centrifuged at room temperature, $18000 \times g$ for 10 min to remove any unwanted precipitate and the clear supernatant was collected and injected into the HPLC to determine DCX released at each time point.

2.7. In vivo studies

2.7.1. Animals and image acquisition

All experiments were performed on immunodeficient BALB/c female nude mice (Janvier laboratories, France) under animal protocol no. 15005AE/07/FUN01/FIS02/JACP1. Mice were housed in specific pathogen-free (SPF) conditions, according to Federation of European Laboratory Animal Science Associations (FELASA) guidelines.

Images were acquired after inducing sedation with isoflurane from XGI-8 Gas Anesthesia Unit (Caliper Life Sciences, USA). Fluorescence ($\lambda_{exc} = 745$ nm/ $\lambda_{em} = 820$ nm) was acquired with IVIS® spectrum imaging system (Caliper Life Sciences, Perkin-Elmer, USA) at different time intervals.

2.7.2. Determination of local residence and biodistribution

To evaluate IP residence and biodistribution of DiNC-PEG gel, 20 mice were divided into 2 sets. The first set of 7 mice were randomized into one of the following groups (n = 2 animals per group): DiR alone, DiNC and DiNC-Fn gel groups, while 1 mouse acts as a negative control, which received isotonic trehalose solution. Second set of 13 mice were randomized into one of the following groups (n = 4 animals per group) DiR alone, DiNC and DiNC-PEG gel groups, while 1 mouse acts as a negative control (isotonic trehalose solution). Whole-body images were captured at 0, 4 and 24 h for the first set, while images for the second set were captured at 0, 4 and 24, 48, 96 h and 1 week after administration. Animals were sacrificed and organs were collected after 24 h for the first set, while it was performed after 1 week for the second set. DiR alone, DiNC and negative control (isotonic trehalose solution) were administered through IP injection (100 µL/mice, 5 ppm DiR concentration), while DiNC-PEG gel was implanted after making a surgical incision of approximately 1 cm over the peritoneal cavity, which was further closed by stainless steel wound clips.

3. Results and discussion

The aim of this work was to develop and characterize a cross-linked PEG hydrogel system containing NCs to improve NC retention after IP administration. This system was characterized *in vitro* and then, the *in vivo* local residence and biodistribution were evaluated using IVIS® imaging in nude mice after IP administration.

3.1. Preparation and characterization of HA NCs

3.1.1. Development and optimization of NCs

NCs were prepared by the self-emulsification method previously described by our group (Fernandez et al., 2016; Štaka et al., 2019). Firstly, a cationic nanoemulsion was prepared with a mixture of oil, surfactant and a positively charged cosurfactant benzethonium chloride. NCs were then formed by electrostatic interaction of the nanoemulsion droplets with an anionic polymer, HA, in an aqueous solution. Three different oils: olive oil, Labrafac and castor oil, were selected to evaluate the solubility of a hydrophobic drug appropriate for peritoneal delivery, DXM, in a range of oils. Olive oil is majorly composed of oleic acid, while Labrafac is rich in caprylic/capric triglycerides and castor oil predominantly consists of ricinoleic acid. Furthermore, Kolliphor® RH 40, Labrasol and Tween® 80, all in the HLB range of 14 to 16 were used as surfactants. Optimization was performed by identifying the potential surfactant and oil that would offer better physical stability, without any phase separation or recrystallization, which was followed by identification of the appropriate concentrations of the surfactant and oil that rendered desired colloidal properties. Initially, to identify the potential surfactant and oil among the above-mentioned ingredients, physical mixtures of surfactant and oil were prepared in water. DXM was incorporated into these mixtures to evaluate relative solubility and recrystallization. Ethanol was used as a cosolvent to dissolve DXM. These physical mixtures were then evaluated for phase separation and optical microscopy after leaving for 24 h (Figure S1 in ESI). Mixtures containing Tween® 80 with olive oil and castor oil showed phase separation. Similarly, mixtures containing Labrasol, with all three oils, showed phase separation. Kolliphor® RH 40 did not show phase separation, while DXM was precipitated from these mixtures, which was not seen with Labrasol and Tween® 80. The physical mixture containing Tween® 80 and Labrafac neither showed phase separation nor recrystallization. Hence, these two ingredients were selected as surfactant and oil for further optimization.

Nanoemulsions were then prepared using Tween® 80 and Labrafac and ethanol in water. As explained above, Kolliphor® RH 40 was successful in the prevention of phase separation with three different oils. Hence, it was evaluated as a co-surfactant. These nanoemulsions were then left undisturbed for 3 days and evaluated for phase separation. The physical state of the nanoemulsion was also recorded to differentiate between the liquid and semisolids that were formed because of the higher concentration of the surfactants. Table S1, in SI, shows the physical stability of nanoemulsions. Nanoemulsions that were semisolid (gel-like) in nature were not considered further because of the foreseeable difficulty in incorporating them in the hydrogels. Nanoemulsions formed with Tween® 80, Labrafac and Kolliphor® RH 40 at a concentration of 20, 10 and 10% w/w, respectively, showed no phase

separation after storage for 3 days and ease of handling, without showing gel-like properties. Hence, this composition was explored for the formation of NCs.

Once the core of the nanoemulsion was optimized, NCs were prepared by electrostatic deposition of an anionic polymer, HA, onto them, as previously reported by our group (Cadete Pires; Fernandez et al., 2016; Oyarzun-Ampuero et al., 2013; Štaka et al., 2019; Storozhylova et al., 2020). With that aim, a positively charged surfactant, benzethonium chloride, was incorporated into the nanoemulsion. In this study, we prepared NCs with two different average molecular weights of HA, 40 kDa and 700 kDa. DXM loaded NCs (DXNC) were prepared and were stored at 2 – 8 °C for 28 days to evaluate the colloidal stability. Fig. 1 shows the mean particle size and PDI of these NCs determined at 1, 4, 7, 14 and 28 days after preparation. Among all the formulations, DXNC prepared with 40 kDa HA at 0.25% w/w showed the best stability in terms of particle size and PDI (Table 1). Moreover, drug loading and its potential leakage were also evaluated after storing the DXNC at 2 – 8 °C for 2 weeks. As shown in ESI, Table S2, it was observed that HA at 0.25% w/w did not show any loss of drug loading. Considering the colloidal stability and a stable drug loading, 40 kDa HA at 0.25% w/w was selected for further studies.

3.1.2. Preparation of DCX loaded NCs

Once NCs preparation was optimized, DCX was incorporated for the potential treatment of peritoneal tumours and entrapment efficiency and drug loading determined. Formulations with 7.5 and 12 mg/mL DCX showed birefringence, indicating the recrystallization of DCX. While no recrystallization was observed at a DCX concentration of 3 mg/mL (Figure S2 in ESI). Table 1 shows the colloidal properties, % EE and drug loading of DCNC. Incorporation of DCX in the NCs was not found to influence its colloidal properties as no change in particle size and PDI was observed. HA NCs first published in our lab has shown a % EE of 65.5 ± 3.1 % (Oyarzun-Ampuero et al., 2013). Although these studies have reported higher % EE than 45% for DCNC, it should be noted that the method of preparation of those NCs was solvent evaporation in contrast to self-emulsification, which was used herein. Self-emulsifying HA NCs reported by Cadete et al. showed % EE of 88 ± 9 %. However, the drug loading achieved with this formulation was 1.8 mg/mL, in contrast to 3.0 mg/mL achieved in the current study (Cadete Pires). Unlike self-emulsification, the solvent evaporation technique involves repeated evaporation cycles, which concentrates the NCs. Self-emulsification is a simpler manufacturing process where evaporation is not required.

Table 1

Colloidal properties of blank NCs, DXNC, DCNC or DiNC at 3 different concentrations of DiR. % EE of DiR was determined by isolating the DiNC immediately after preparation, followed by extracting the DiR in ethanol and quantifying the fluorescence at an emission wavelength of 785 nm. DCX was extracted in ethanol, followed by HPLC analysis with UV detection at 227 nm. Each value is represented as mean ± SD (n = 3).

Sample	Size (nm)	PDI	Zeta potential (mV)	% EE	Drug loading (% w/w)
Blank NCs	250 ± 30	0.2	−17 ± 3	–	–
DXNC	220 ± 22	0.2	−17 ± 3	46 ± 6	5.3 ± 0.1
DCNC	235 ± 20	0.2	−17 ± 2	45 ± 5	3.0 ± 0.3
90 ppm DiNC	200 ± 15	0.2	−17 ± 3	42 ± 6	–
120 ppm DiNC	181 ± 10	0.2	−17 ± 3	46 ± 5	–
180 ppm DiNC	174 ± 15	0.2	−17 ± 3	42 ± 4	–

3.1.3. Incorporation of DiR into HA NCs

DiR, a near-infrared dye, was incorporated into the NCs to assist *in vivo* tracking upon IP administration. The longer emission wavelength of DiR favours whole-body imaging of animals without the influence of autofluorescence (Xu et al., 2015). Particle size, PDI and zeta potential were measured after incorporation of DIR. Although statistically insignificant, interestingly, DiR concentration showed some inconsistencies in the particle size, while PDI and zeta potential were unchanged. It was observed that DiNC with the highest DiR concentration had the lowest particle size. These differences in particle size could be attributed to the amphiphilic properties of DiR which was observed by Bastiat et al, where the use of near IR fluorescent dyes, DiI and DiO, showed a reduction in the interfacial tension between Labrafac and water, demonstrating their amphiphilic surfactant-like properties (Bastiat et al., 2013).

Table 1 shows the % EE of DiR. It was observed that 42 – 46 % of DiR was entrapped into NCs, irrespective of the initial concentration of DiR in the tested concentration range. Percentage recovery, calculated by comparing the theoretical concentration of DiR against the sum of entrapped and unentrapped DiR, was > 90 %.

3.2. Preparation and characterization of NCs loaded hydrogels

Having optimized NCs to incorporate DCX and DiR, a covalently cross-linked PEG gel was developed to incorporate these NCs for IP administration and NC retention at the administration site.
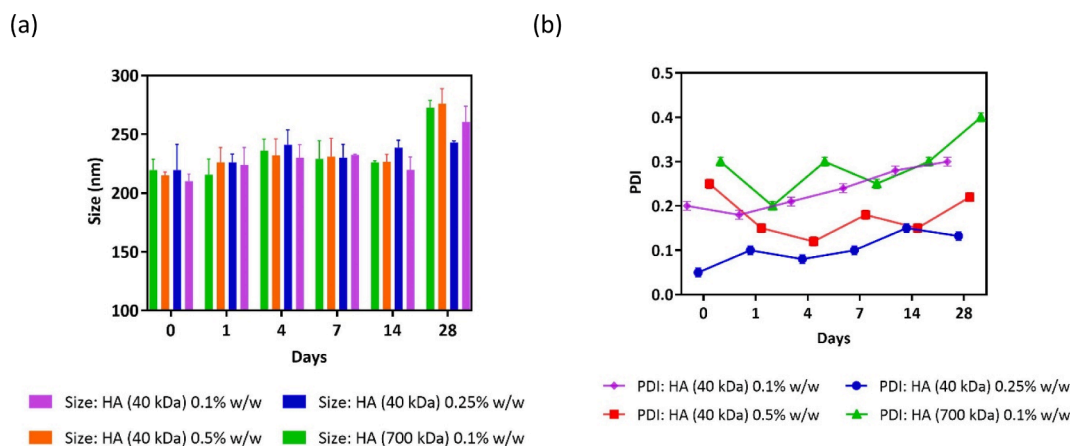

Fig. 1. Influence of the molecular weight and concentration of HA on the colloidal stability of DCX NCs. (a) Particle size and (b) PDI were measured after preparing the NCs and at different time points during their storage at 2–8 °C. HA (40 kDa) at 0.25% w/w showed relative stability, while other formulations showed an increase in size after 28-day storage (p < 0.05, Dunnett's multiple comparison test). (Each value is a mean ± SD of 3 preparations).

Development of the hydrogel aimed to incorporate at least 30% w/w of NCs, which would yield a DCX dose of 7.2 mg/kg (based upon the maximum amount of hydrogel that can be administered to the mouse IP cavity i.e. 200 µL). The 7.2 mg/kg dose is comparable to doses reported in other preclinical studies (Shimada et al., 2005; Yonemura et al., 2004).

3.2.1. Development of covalently cross-linked PEG gels

Covalently cross-linked hydrogels were developed via thiol-Michael addition between a PEG-MAL and a PEG-SH as a crosslinker. Due to their high reaction efficiency, cross-linked PEG-MAL hydrogels can be obtained without requiring the use of additional catalysts (Darling et al., 2016; Foster et al., 2017; Jansen et al., 2018). Given their high versatility and biocompatibility, PEG-based hydrogels prepared via thiol-Michael addition have been widely used for biomedical applications, such as protein and cell delivery, regenerative medicine, and injectable hydrogel scaffolds (Baldwin and Kiick, 2013; García, 2014; Griffin et al., 2015; Phelps et al., 2015). PEG gels have also been explored for local drug delivery. Yu et al. incorporated Avastin® into a covalently cross-linked 4-arm PEG-MAL and 4-arm PEG-SH (20 kDa) hydrogel, achieving a sustained drug delivery up to 14 days *in vitro*, with no apparent cytotoxicity (Yu et al., 2014). Modification of covalent linkers in order to tune hydrolysis and degradation rate of hydrogels is a widely reported strategy in the literature to control drug release (Schoenmakers et al., 2004; Zustiak and Leach, 2011). However, according to our knowledge, PEG gels incorporating NCs have not been reported. Herein, we have first synthesised PEG-SH via esterification of a linear PEG with 3-mercaptopropionic acid. This reaction incorporated ester groups as part of the cross-linker which are susceptible to degradation by hydrolysis (Zustiak and Leach, 2010). This will favour hydrogel degradation *in vivo*, which would control drug release and render biodegradability to the formulation (Jain et al., 2017). Free -SH groups on the PEG-SH cross-linker, react with PEG-MAL to form a hydrogel as shown in Figure S4 in ESI.

The rate of Michael addition reaction is influenced by the pH of the medium. Jansen et al. reported that reduction in the pH of the medium reduces the reaction kinetics, which was due to the base catalysis of nucleophilic addition onto alkene group of maleimide, which favoured the formation of stable polymeric networks (Jansen et al., 2018). Strong bases such as triethanolamine (pKa 7.76) catalyze the reaction much faster than weak acids such as a citrate buffer (pKa 6.40). However, faster reaction kinetics is not favourable to ensure homogeneity of the gel components during mixing (Darling et al., 2016). Moreover, lower pH can be challenging to ensure the colloidal stability of the NCs. Hence, an optimum pH needs to be identified. DiNC were incubated in various buffers, ranging from pH 3 to 6 at 25 ± 5 °C for 2 h and colloidal properties were analyzed. It was observed that lowering the pH of the buffer until pH 4 did not significantly change the particle size and PDI of the NCs. Interestingly, 0.1 M citrate buffer at pH 3.0, destabilized the DiNC, resulting in increased particle size and PDI. This could be due to the perturbation of electrostatic interactions between benzethonium chloride and HA. As pH 4.0 was the lowest possible threshold to obtain a hydrogel with stable NCs, a slightly higher pH of 5.0 was chosen for further gel preparation. Table 2 shows the particle size and PDI of DiNC measured after incubation in different pH buffers.

Table 2
Determination of colloidal stability of DiNC up on incubation in buffers with different pH, at 25 ± 5 °C for 2 h. Data is represented as mean ± SD (n = 3).

Incubation medium	Size (nm)	PDI
Milli-Q water	243 ± 18	0.1
PBS (0.01 M, pH 7.4)	230 ± 15	0.1
Citrate buffer (0.1 M, pH 6)	228 ± 38	0.1
Citrate buffer (0.1 M, pH 5)	221 ± 20	0.1
Citrate buffer (0.1 M, pH 4)	226 ± 28	0.1
Citrate buffer (0.1 M, pH 3)	449 ± 80	0.3

3.2.2. Preparation of Fn-HA hydrogel comparator

We have previously described a Fn-HA gel, which could incorporate NCs loaded with an antagonist for galactin-3, a proinflammatory cascade initiator, for the treatment of rheumatoid arthritis (Storozhylova, 2018). In this study, we have adapted this Fn-HA gel, a physically cross-linked hydrogel, to incorporate NCs. Fibrinogen (24% w/w), thrombin (8% w/w) and a mixture of HAs (34% w/w) was used to incorporate 30% w/w NCs. DiNC was also incorporated into Fn-HA gel as described above. This gel was used to develop the *in vivo* fluorescence imaging methodology using IVIS®.

3.2.3. Rheology

Oscillatory rheology studies were performed on NC-Fn and NC-PEG gels to confirm hydrogel formation. The storage modulus (G', elastic, solid-like behaviour) and the loss modulus (G", flow properties, liquid-like behaviour) of NC-Fn gel were recorded using oscillatory amplitude sweeps. Hydrogel formation was confirmed by a G' higher than G" in the linear viscoelastic (LVE) regime (from 0.01% to 4%) as shown in Fig. 2a. The storage modulus derived from the LVE of the amplitude sweep test was used as a measure of NC-Fn gel strength, with a value of 61 ± 6 Pa, which is comparable to similar Fn-HA gels reported by Storozhylova et al. (Storozhylova et al., 2020).

Gelation kinetics of NC-PEG gel was evaluated by following the change in storage (G') and loss modulus (G") with time, in order to guarantee the selected buffer pH (5.0) was adequate for gelation. G' and G" were found to gradually increase with time as shown in Fig. 2b. The crossover point of G' over G" is conventionally used to determine the onset of gelation (Aimetti et al., 2009; Darling et al., 2016), and no crossover point of G' and G" was observed, indicating the initiation of gelation occurred immediately after the components mixing. As the gels were prepared at pH 5.0, gelation kinetics are expected to be rapid, which did not reveal the crossover point under the experimental conditions (Jansen et al., 2018). Further reduction in pH of the preparation buffer could reduce the gelation time. However, colloidal properties of NC would be compromised at further lower pH (pH < 4). The highest G' of 548 ± 150 Pa was seen at 30 min.

Higher mechanical strength would help to withstand the dynamic environment in IP cavity. For example, Yeo et al., reported a G' value of 420 Pa for their a composite gel of poly (lactic-coglycolic acid) (PLGA) NPs in a covalently cross-linked HA hydrogel that prolonged NC retention to one week in the peritoneal cavity. They reported for their gels a G' 420 Pa, which is comparable to the G' of the NC-PEG gel herein of 548 Pa (Yeo et al., 2007). Hence the cross-linked PEG hydrogel has the appropriate mechanical strength for retention within the peritoneal cavity. Furthermore, another covalently crosslinked hydrogel prepared by crosslinking N, O-carboxymethyl chitosan and aldehyde HA was found to be retained for up to 2 weeks in rats after IP administration. G' and G" of this hydrogel, as observed from gelation kinetics experiments, were found to be approximately 10 fold lower than NC-PEG gel (Li et al., 2014).

3.2.4. Resistance to dilution

The IP cavity is a dynamic environment with high fluid turnover rates, causing small and large molecules to be cleared rapidly from the cavity (Flessner, 1991). Hydrogels and other depot drug delivery systems also face a similar challenge of rapid clearance because of these high fluid turnover rates (Bajaj and Yeo, 2010). Accordingly, it is very important to evaluate the resistance of hydrogels to dissolution at high dilutions. Bajaj et al. observed that covalently cross-linked HA gels were resistant to dilution in a IP relevant buffer and gave slow degradation over 10 days, leading to paclitaxel release profiles from nanocrystals suitable for an *in vivo* anti-tumour effect (Bajaj et al., 2012). In this study, we evaluated the resistance to dissolution after exposing both NC-Fn and NC-PEG gels to 1:3 to 1:25 dilutions in SIPF at 37 °C. Upon visual observation, gels that were swollen but remain undissolved as intact gels in the media were considered to have tolerance to dilution. NC-Fn gel
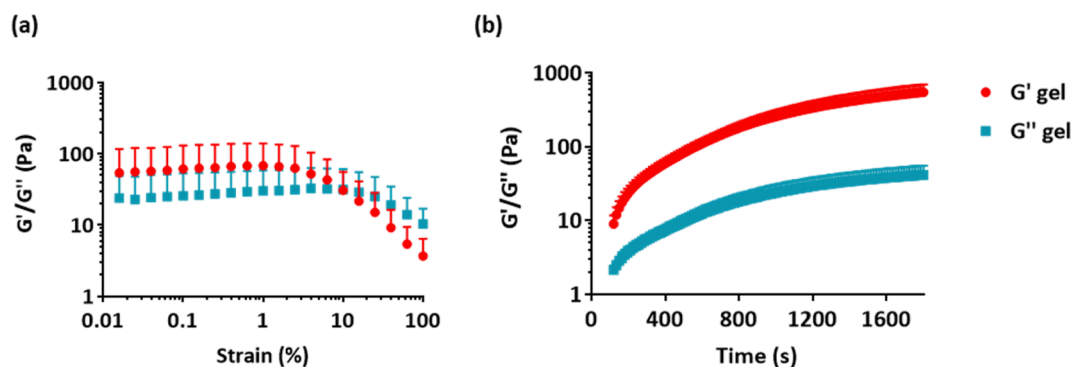
Fig. 2. Rheology performed on NC-Fn and NC-PEG gels. (a) Oscillatory amplitude sweeps of NC-Fn gel performed within the strain range of 0.1 to 100 % at a fixed frequency of 10 rad s^{-1}, 25 °C. (b) Gelation kinetics of NC-PEG gel as determined by oscillatory rheology performed on parallel plate assembly at 20 rad s^{-1} frequency, 0.5% strain, and 25 °C, showing the increase of G' and G'' with time. Data represented as mean $\pm$ SD (n = 3).

tolerated a 1:3 dilution only, showing complete dissolution at 1:9 and 1:25 dilutions. NC-PEG gels were incubated with SIPF at 37 °C, at 5% and 10% w/w concentrations of PEG-MAL. Both 5 and 10% w/w gels were swollen initially and occupied the whole media at 1:3 and 1:9 dilutions and remained intact (SI Figure S5). Interestingly, gels containing 10% w/w PEG-MAL remained intact for up to 3 weeks, while gels containing 5% w/w PEG-MAL were intact for up to 2 weeks at 1:25 dilution. Higher resistance to dilution would be favourable for longer retention in the IP cavity, as it would help the formulation to withstand the high fluid turnover rates. Physically assembled hydrogels dissociate rapidly through dissolution in aqueous environments (Vintiloiu and Leroux, 2008). In contrast, covalently cross-linked systems cannot be diluted and instead swell. A covalently cross-linked HA gel containing cisplatin was reported to be retained after 28 days following IP administration (Emoto et al., 2014). With being chemically cross-linked, the NC-PEG gel would have a high potential to be retained longer than NC-Fn gel in the IP cavity.

3.2.5. In vitro release studies

After determining the resistance to dilution, it was then necessary to follow the degradation of both these gels where the gels remains intact i. e 1:3 for DiNC-Fn or where it does not occupy the whole media due to

Fig. 3. In vitro release study showing the % cumulative release of DiR from DiNC-Fn and DiNC-PEG gels, as estimated by fluorescence analysis from each time point. DIR was incorporated into the NCs. Gels were prepared incorporating 30% w/w of DiNC. DiNC-Fn gel was incubated under 1:3 dilution in SIPF at 37 °C, while DiNC-PEG gels, prepared at 5 and 10% w/w concentrations of PEG-MAL and equimolar concentrations of PEG-SH, were incubated under 1:25 dilution in SIPF at 37 °C. Data represented as mean $\pm$ SD (n = 3).

swelling i.e 1:25 for DiNC-PEG gel. As shown in Fig. 3, DiNC-Fn gel showed a gradual release up to 40 % in 48 h at 1:3 dilution. However, complete DiR release from the hydrogel was observed at 72 h. This could be attributed to the relatively weak interactions associated with physically assembled hydrogels. The formation of loose networks upon dilution cannot hold the NCs within the hydrogel, leading to their release into the media. Although DiNC-Fn gel showed slower release at 1:3 dilution throughout 72 h, this release profile would not be appropriate in a dynamic IP environment and would require repeated dosing.

In contrast, DiNC-PEG gels containing 5 and 10% w/w PEG-MAL showed a cumulative release of approximately 80% and 45% after 5 days respectively. Gels were physically retained after the study, showing > 85% recovery of the remaining DiR. In addition, very similar release data was obtained for DCX containing nanocapsules when loaded into a 10% w/w PEG-MAL, where 45% of DCX was released from the gel within 24 h, which remained consistent over 48 h (SI Figure S6). It should be noted that the release profile is indicative of the sum of free drug/dye and NCs with drug or dye released into the media, as isolation of NCs from the medium, either by centrifugation or size exclusion columns, led to their destabilization. The presence of NCs in the release media was confirmed by obtaining DLS measurements of the media after incubation with DiNC-PEG gel.

Interestingly, the total release obtained with DiNC-PEG gel containing 10% w/w PEG-MAL showed only 40% release in 24 h, which was consistent over 5 days. While, DiNC-PEG gel containing 5% w/w PEG-MAL showed 70% release in 24 h, which plateaued over 5 days. The higher concentration of polymer and crosslinker provides higher cross-linking density for DiNC-PEG gel containing 10% w/w PEG-MAL, which would further control the release from the hydrogel (Lee et al., 2016). The initial burst release from both DiNC-PEG gels with 10% w/w and 5% w/w PEG-MAL could be attributed to the diffusion of DiR or release of NCs from the hydrogel due to initial swelling and an increase in the pore size. Thereafter release of NCs occurs in tandem with the degradation of the hydrogel. As discussed earlier, DiNC-PEG gel will degrade via ester hydrolysis (Schoenmakers et al., 2004). SIPF is an aqueous media, which was under constant stirring and replacement during the study. Such fluid dynamics might favour ester hydrolysis, eventually degrading the gel, which further releases NCs into the media. However, in vivo degradation is likely to be influenced by other factors such as the presence of enzymes and protein filtrates from blood in the ascites fluid.

Based on resistance to dilution and in vitro release studies, the DiNC-PEG gel containing 10% w/w PEG-MAL demonstrated superior performance to its 5% w/w equivalent and DiNC-Fn gel. Hence, a 10% w/w PEG-MAL concentration was chosen to progress to in vivo studies.
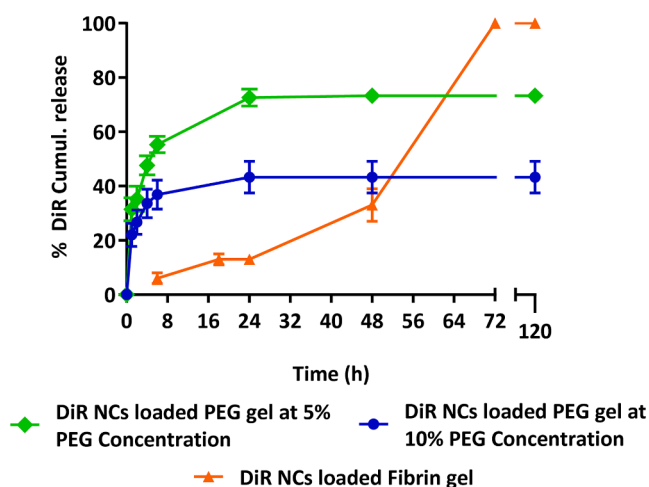
3.3. In vivo studies

3.3.1. Development of IVIS® using IP residence of DiNC-Fn gel

Initially two pilot studies were conducted to determine a suitable of concentration of the fluorescent dye DIR in the NC for IVIS® imaging (SI

Figure S7). Local residence and biodistribution of DiNC and DiNC-Fn gel was then studied as shown in SI Figure S8. Mice administered with DiNC or DiNC-Fn gel showed some fluorescence from the abdominal cavity up to 2 weeks. The fluorescence could come from the IP cavity or from the liver, since it has been well documented that nanoparticulate drug
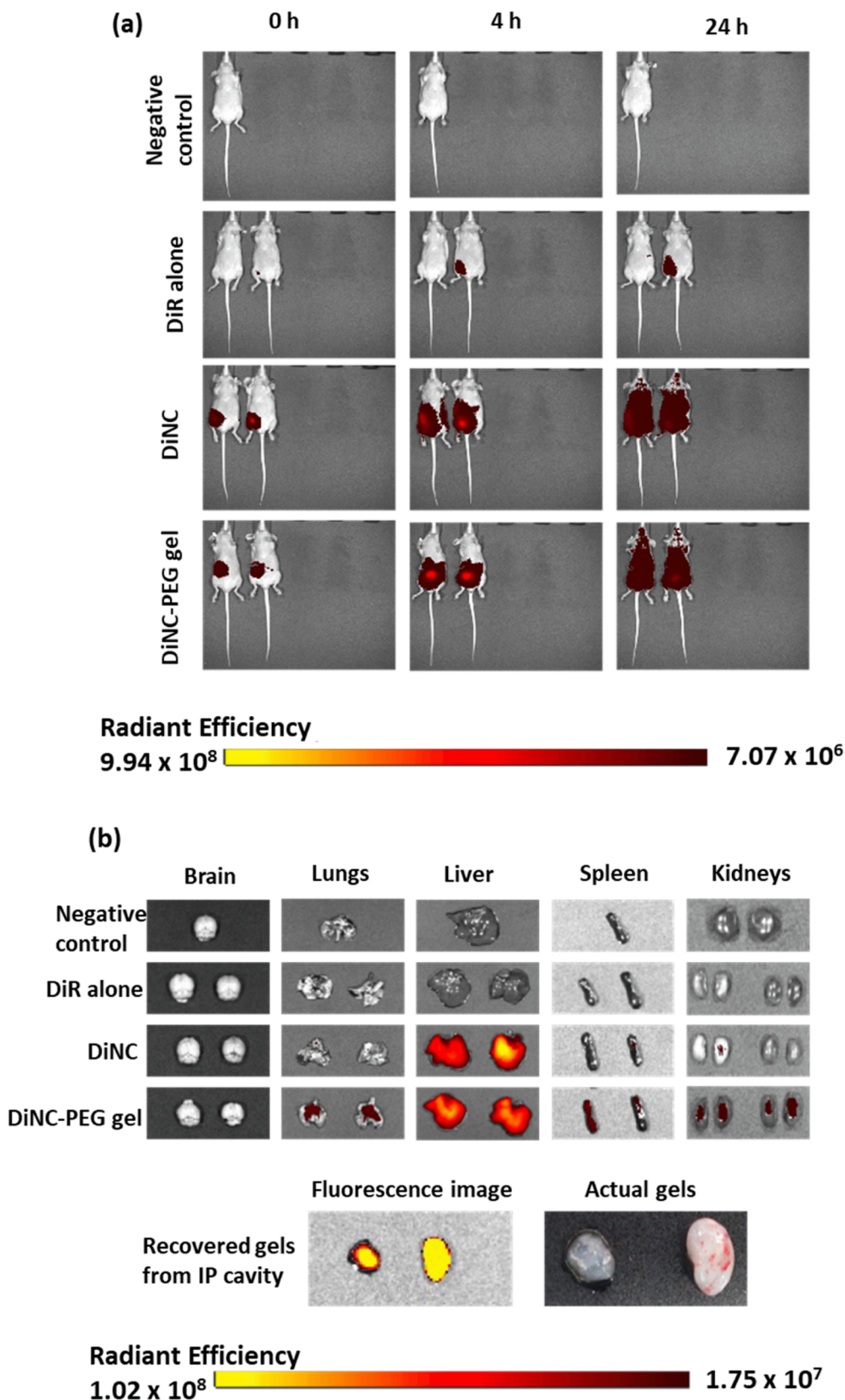
Fig. 4. In vivo IVIS® imaging study performed on mice (set 1) (a) Compilation of images acquired after 0, 4 and 24 h of administration, showing the fluorescence obtained from DiR alone, DiNC and DiNC-PEG gel groups. Mouse administered with isotonic trehalose solution as negative control is also represented in the image. (b) Compilation of images acquired from organs obtained after sacrificing the mice at 24 h time point, showing the fluorescence prominently from liver in case of DiNC and DiNC-PEG gel groups. Gels retrieved from the peritoneal cavity after 24 h, indicating the fluorescence, are also shown here.

delivery systems can drain through capillary lymph vessels upon IP administration, entering the systemic circulation and then be removed by macrophages of the liver (Kohane et al., 2006; Yang et al., 2013). Hence, whole organs were imaged to capture the fluorescence (Figure SI 8b). As expected, the liver showed fluorescence while other organs did not show any signal. As IVIS® is a qualitative technique, it was difficult to estimate the relative proportion of fluorescence from the IP cavity and the liver at the end of the study. Moreover, the study has highlighted the difficulties in interpreting whole body fluorescence imaging data when evaluating IP administration and the necessity to image the fluorescence intensity of individual organs and any gel remaining in the cavity.

3.3.2. IP residence and biodistribution of DiNC-PEG gel

After understanding the difficulties in interpretation of *in vivo* biodistribution, the study to determine the IP retention of NCs within the PEG gel included earlier time points and gels recovered from the cavity. Hence, animals were classified into two sets in order to obtain biodistribution data at these earlier time points.

Fig. 4a shows the compilation of images of the first set of mice,

captured from the ventral side. Fluorescence was emitted from the site of administration for up to 24 h. The images showed significant fluorescence in the gel recovered from the peritoneal cavity at 24 h, thus suggesting the retention of the hydrogel containing DiNC (Fig. 4b). To treat any locoregional disease associated with the peritoneal cavity, the retention of nanocapsules herein gives a method whereby drug loaded nanocapsules could be retained in the cavity giving a localised drug concentration.

Even though there was evidence of nanocapsules retained in the cavity by the hydrogel, surprisingly the biodistribution pattern of DiNC was similar with and without the hydrogel, and indicated that DiNC were preferentially taken up by the liver as previously observed for the DiNC FN-gel. In fact, it is well known in the literature as previously described that NPs tend to escape rapidly from the peritoneal cavity through both lymph duct and capillary endings. For example, Mirahmadi describe only 9.0% retention in the peritoneal cavity of a 100 nm negatively charged liposome formulation after 7 h(Mirahmadi et al., 2010). Hence, we would anticipate that most of the negatively charged nanocapsules not retained in the gel would drain through the lymphatics
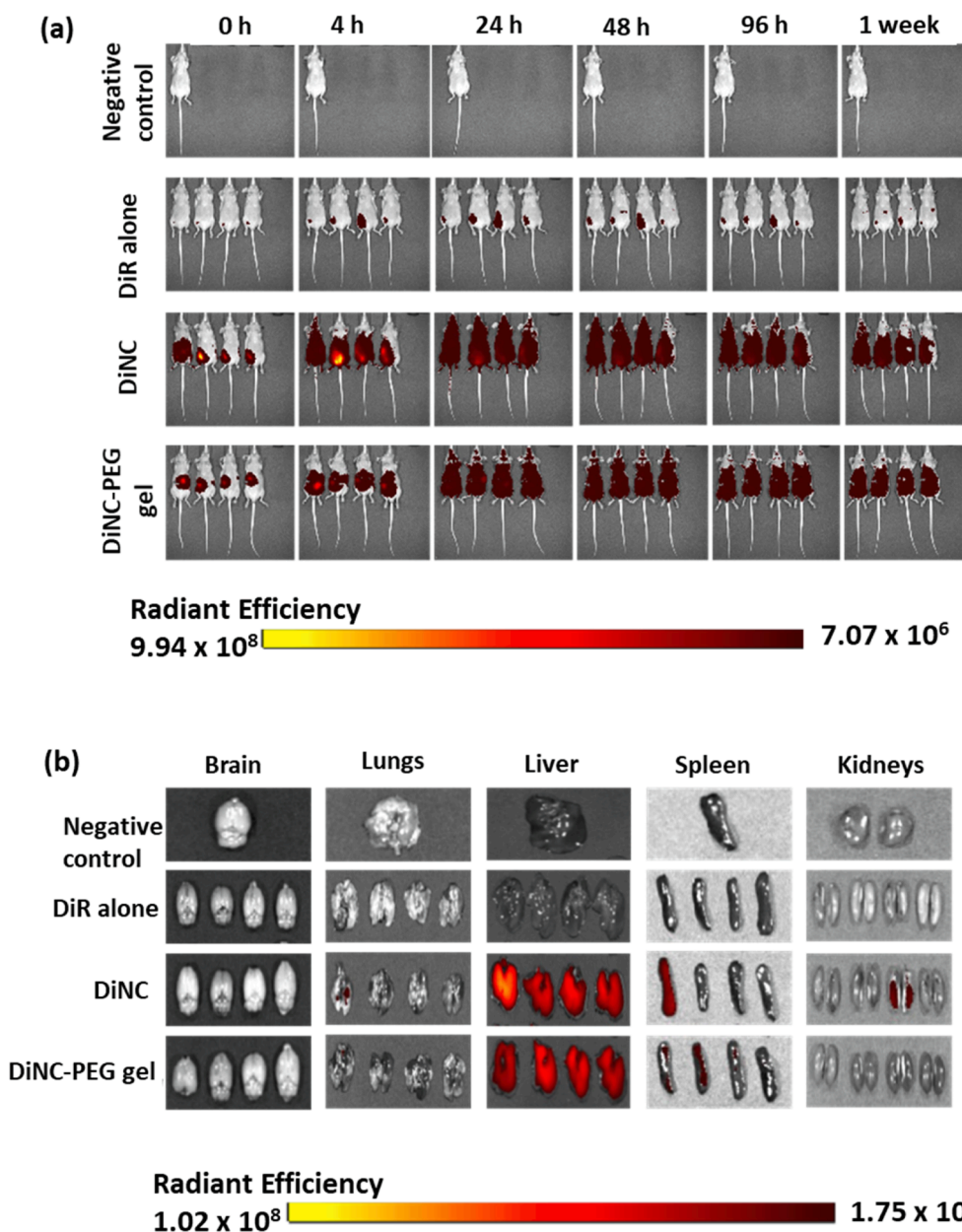

Fig. 5. In vivo IVIS® imaging study performed on mice (set 2) (a) Compilation of images acquired after 0, 4, 24, 48, 96 h and 1 week of administration, showing the fluorescence obtained from DiR alone, DiNC and DiNC-PEG gel groups. Mouse administered with isotonic trehalose solution as negative control is also represented in the image (b) Compilation of images acquired from organs obtained after sacrificing the mice at 1 week time point, showing the fluorescence prominently from liver in case of DiNC and DiNC-PEG gel groups. No gel was retained in the IP cavity after 1 week.

into the systemic circulation and be sequestered by the macrophages in the liver by 24 h timepoint. Also Tsai *et al* report <0.01% of the dose of a paclitaxel gelatin loaded nanoparticle remaining in the peritoneal cavity after 24 h(Tsai et al., 2007). Differences in biodistribution may have been evident at earlier time points. However, there is a scarcity of biodistribution data for nanocomposite hydrogels which to compare our data herein. In contrast, there are numerous reports of nanoparticle and microparticle biodistribution studies after peritoneal administration (examples above) and there are reports of hydrogels administered in combination with chemotherapeutics giving efficacy in ovarian cancer tumour models (Dakwar et al., 2017). Indeed, there are no clear hypotheses that can explain this similarity in biodistribution in the liver between nanocapsules alone and hydrogel with nanocapsules at 24 h but still having nanocapsules retained by the hydrogel in the cavity. For example, saturation of uptake by macrophages of the liver seems unlikely(Ngo et al., 2022).

As the retention of DiNC-PEG gel was confirmed after 24 h, gel retention in the cavity up to 1 week was also assessed. Fig. 5a shows the compilation of a set of 2 images, sacrificed after 1 week. Interestingly, no traces of hydrogel were found in the IP cavity, indicating that the hydrogel was completely degraded between 24 h and 1 week. The dynamic, fluid rich IP cavity may have degraded the gel through ester hydrolysis and enzymatic degradation. Moreover, the thioether formed by the Michael addition could undergo degradation *in vivo* via thiol-exchange reaction and also, to a lesser extent, ring-opening hydrolysis in biological environments (Fontaine et al., 2014).

Biodistribution after 1 week showed a similar pattern to 24 h, both similar but lower average radiance from the liver (Fig. 5b). However, no traces of hydrogel were observed in the peritoneal cavity. Based on this data, it can be concluded that the DiNC-PEG gel was retained in the IP cavity between 24 h and 1 week, while DiNC escaped from the cavity and accumulated in the liver after being released from the hydrogel. In comparison to the *in vitro* release study, where DiNC-PEG gel showed approximately 40% release in the SIPF up to 5 days after incubation, *in vivo* degradation, was rapid, demonstrating the complete degradation within a week. This could be due to the high fluid turnover rate present in the IP cavity, which is difficult to replicate *in vitro*. Fig. 6 also shows that the radiant efficiency from the liver after 1 week was similar to that of the 24 h time point, which further supports the liver accumulation. No significant fluorescence was observed from kidneys, which indicated that neither DiR nor DiNC was eliminated through urine. Schädlich *et al.* reported the excretion of DiR and DiR-loaded PEG-PLA NPs through bioconjugation in the liver, followed by excretion via gall into intestine, eventually clearing through faeces. They confirmed the faecal excretion through the presence of fluorescence in the intestine (Schädlich et al.,

2011). Interestingly, fluorescence was also seen in the lungs after 24 h, as observed with DiNC-PEG gel group (Fig. 4(b)). This might be due to macrophage-assisted migration of NCs to the lung tissue, after IP administration. Parayath *et al.* demonstrated the macrophage-specific targeting of HA NPs through CD44 residues, which favoured the accumulation of NPs in lung tissue after IP administration (Parayath et al., 2018).

This study demonstrates the biodegradability of PEG gel in the IP cavity of mice. In addition, PEG MAL based gels have been shown to be non-toxic when implanted *in vivo* (Phelps et al., 2012). Further evidence of the non-toxic nature of PEG-MAL gel used in this study and cross-linked with a dithiol PEG ester is the work by Kroger *et al*. They have shown that these gels can be used for cell encapsulation with high cell viability and that cell viability is also high upon exposure to leachables and degradation products from the gel (Kroger et al., 2020).

In summary, this NC containing PEG hydrogel shows potential for progression to preclinical efficacy studies in an ovarian cancer model as there is evidence of retention of the hydrogel with nanocapsules at 24 h. We envisage that ultimately NCs containing chemotherapeutics in a PEG gel could be placed as an implant in the tumour resection cavity by a surgeon after cytoreductive surgery, to target microscopic, metastatic remnant tumour nodules.

4. Conclusion

The primary focus of this study was the development, characterization and evaluation of a covalently cross-linked PEG gel containing NCs for IP drug delivery. In vitro data demonstrated that for the first time NCs could be successfully encapsulated within a cross-linked PEG gel and slowly released. Using IVIS® to measure individual organ and recovered gel fluorescence intensity, an *in vivo* imaging study was performed and demonstrated that NCs incorporated in the PEG gel were retained in the IP cavity for 24 h after IP administration. NCs-loaded PEG gels could find potential applications as biodegradable, drug delivery systems that could be implanted in the IP cavity, for example at a tumour resection site to prevent recurrence of microscopic tumours.
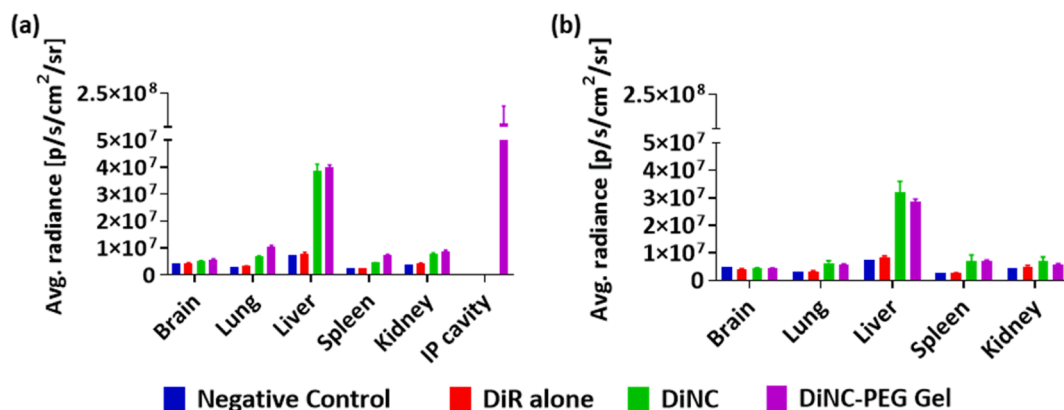
Fig. 6. Biodistribution obtained from IVIS® imaging study after administration of negative control, DiR alone, DiNC and DiNC-PEG gel after IP administration. (a) Average radiance obtained from various organs acquired after sacrificing the mice at 24 h after IP administration. IP cavity has shown remnants of DiNC-PEG gel, whose average radiance is also represented here. Data represented is mean ± SEM (n = 2). (b) Average radiance obtained from various organs acquired after sacrificing the mice at 1 week after IP administration. No remnants of gel was found in the IP cavity after 1 week. Data represented is mean ± SEM (n = 4).

Supervision, Formal analysis, Writing – review & editing, Project administration, Funding acquisition. **Irene Golán Cancela:** Investigation, Methodology, Formal analysis, Writing – review & editing. **José A. Costoya:** Conceptualization, Resources, Methodology, Visualization, Supervision, Formal analysis, Writing – review & editing, Project administration. **José Crecente Campo:** Conceptualization, Resources, Methodology, Visualization, Supervision, Formal analysis, Writing – review & editing, Project administration. **Maria José Alonso:** Conceptualization, Resources, Methodology, Visualization, Supervision, Formal analysis, Writing – review & editing, Project administration, Funding acquisition. **Maria Marlow:** Conceptualization, Resources, Methodology, Visualization, Supervision, Formal analysis, Writing – review & editing, Project administration, Funding acquisition.

Declaration of Competing Interest

The authors declare that they have no known competing financial interests or personal relationships that could have appeared to influence the work reported in this paper.

Acknowledgements

Appendix A. Supplementary material

Supplementary data to this article can be found online at https://doi.org/10.1016/j.ijpharm.2022.121828.

References

Aimetti, A.A., Machen, A.J., Anseth, K.S., 2009. Poly (ethylene glycol) hydrogels formed by thiol-ene photopolymerization for enzyme-responsive protein delivery. Biomaterials 30 (30), 6048–6054.

Amoozgar, Z., Wang, L., Brandstoetter, T., Wallis, S.S., Wilson, E.M., Goldberg, M.S., 2014. Dual-layer surface coating of PLGA-based nanoparticles provides slow-release drug delivery to achieve metronomic therapy in a paclitaxel-resistant murine ovarian cancer model. Biomacromolecules 15 (11), 4187–4194.

Armstrong, D.K., Bundy, B., Wenzel, L., Huang, H.Q., Baergen, R., Lele, S., Copeland, L.J., Walker, J.L., Burger, R.A., 2006. Intraperitoneal cisplatin and paclitaxel in ovarian cancer. N. Engl. J. Med. 354 (1), 34–43.

Bajaj, G., Kim, M.R., Mohammed, S.I., Yeo, Y., 2012. Hyaluronic acid-based hydrogel for regional delivery of paclitaxel to intraperitoneal tumors. J. Control. Release 158 (3), 386–392.

Bajaj, G., Yeo, Y., 2010. Drug delivery systems for intraperitoneal therapy. Pharm. Res. 27 (5), 735–738.

Baldwin, A.D., Kiick, K.L., 2013. Reversible maleimide–thiol adducts yield glutathione-sensitive poly (ethylene glycol)–heparin hydrogels. Polym. Chem. 4 (1), 133–143.

Bastiat, G., Pritz, C.O., Roider, C., Fouchet, F., Lignières, E., Jesacher, A., Glueckert, R., Ritsch-Marte, M., Schrott-Fischer, A., Saulnier, P., Benoit, J.-P., 2013. A new tool to ensure the fluorescent dye labeling stability of nanocarriers: a real challenge for fluorescence imaging. J. Control. Release 170 (3), 334–342.

Bijelic, L., Yan, T.D., Sugarbaker, P.H., 2007. Failure analysis of recurrent disease following complete cytoreduction and perioperative intraperitoneal chemotherapy in patients with peritoneal carcinomatosis from colorectal cancer. Ann. Surg. Oncol. 14 (8), 2281–2288.

Cadete Pires, A., Hyaluronic acid nanocapsules for the intracellular delivery of anticancer drugs.

Ceelen, W.P., Flessner, M.F., 2010. Intraperitoneal therapy for peritoneal tumors: biophysics and clinical evidence. Nat. Rev. Clin. Oncol. 7 (2), 108–115.

Chen, C.-H., Kuo, C.-Y., Chen, S.-H., Mao, S.-H., Chang, C.-Y., Shalumon, K., Chen, J.-P., 2018. Thermosensitive Injectable Hydrogel for Simultaneous Intraperitoneal Delivery of Doxorubicin and Prevention of Peritoneal Adhesion. Int. J. Mol. Sci. 19 (5), 1373. https://doi.org/10.3390/ijms19051373.

Dakwar, G.R., Shariati, M., Willaert, W., Ceelen, W., De Smedt, S.C., Remaut, K., 2017. Nanomedicine-based intraperitoneal therapy for the treatment of peritoneal carcinomatosis — Mission possible? Adv. Drug Deliv. Rev. 108, 13–24.

Darling, N.J., Hung, Y.-S., Sharma, S., Segura, T., 2016. Controlling the kinetics of thiol-maleimide Michael-type addition gelation kinetics for the generation of homogenous poly (ethylene glycol) hydrogels. Biomaterials 101, 199–206.

De Smet, L., Colin, P., Ceelen, W., Bracke, M., Van Bocxlaer, J., Remon, J.P., Vervaet, C., 2012. Development of a nanocrystalline Paclitaxel formulation for HIPEC treatment. Pharm. Res. 29 (9), 2398–2406.

Dedrick, R.L., Flessner, M.F., 1997. Pharmacokinetic problems in peritoneal drug administration: tissue penetration and surface exposure. J. Natl Cancer Inst. 89 (7), 480–487.

Dedrick, R.L., Myers, C.E., Bungay, P.M., DeVita, V., 1978. Pharmacokinetic rationale for peritoneal drug administration. Cancer Treat Rep 62, 1–13.

El-Kamel, R.S., Ghoneim, A.A., Fekry, A.M., 2019. Electrochemical, biodegradation and cytotoxicity of graphene oxide nanoparticles/polythreonine as a novel nano-coating on AZ91E Mg alloy staple in gastrectomy surgery. Mater. Sci. Eng., C 103, 109780. https://doi.org/10.1016/j.msec.2019.109780.

Emoto, S., Yamaguchi, H., Kamei, T., Ishigami, H., Suhara, T., Suzuki, Y., Ito, T., Kitayama, J., Watanabe, T., 2014. Intraperitoneal administration of cisplatin via an in situ cross-linkable hyaluronic acid-based hydrogel for peritoneal dissemination of gastric cancer. Surg. Today 44 (5), 919–926.

Ernsting, M.J., Murakami, M., Roy, A., Li, S.-D., 2013. Factors controlling the pharmacokinetics, biodistribution and intratumoral penetration of nanoparticles. J. Control. Release 172 (3), 782–794.

Fan, R., Tong, A., Li, X., Gao, X., Mei, L., Zhou, L., Zhang, X., You, C., Guo, G., 2015. Enhanced antitumor effects by docetaxel/LL37-loaded thermosensitive hydrogel nanoparticles in peritoneal carcinomatosis of colorectal cancer. Int. J. Nanomed. 10, 7291.

Feldman, G.B., Knapp, R.C., Order, S.E., Hellman, S., 1972. The role of lymphatic obstruction in the formation of ascites in a murine ovarian carcinoma. Cancer Res. 32, 1663–1666.

Fernandez, M.J.A., Lopez, D.T., Rodriguez, G.R., Ampuero, F.A.O., Lollo, G., Lázaro, T. G., Fuentes, M.G., 2016. Nanocapsules with a polymer shell. Google Patents.

Flessner, M.F., 1991. Peritoneal transport physiology: insights from basic research. J. Am. Soc. Nephrol. 2 (2), 122–135.

Flessner, M.F., 2005. The transport barrier in intraperitoneal therapy. Am. J. Physiol. Renal Physiol. 288 (3), F433–F442.

Fontaine, S.D., Reid, R., Robinson, L., Ashley, G.W., Santi, D.V., 2014. Long-term stabilization of maleimide–thiol conjugates. Bioconjug. Chem. 26 (1), 145–152.

Foster, G.A., Headen, D.M., González-García, C., Salmerón-Sánchez, M., Shirwan, H., García, A.J., 2017. Protease-degradable microgels for protein delivery for vascularization. Biomaterials 113, 170–175.

García, A.J., 2014. PEG–maleimide hydrogels for protein and cell delivery in regenerative medicine. Ann. Biomed. Eng. 42 (2), 312–322.

Glehen, O., Kwiatkowski, F., Sugarbaker, P.H., Elias, D., Levine, E.A., De Simone, M., Barone, R., Yonemura, Y., Cavaliere, F., Quenet, F., Gutman, M., Tentes, A.A.K., Lorimier, G., Bernard, J.L., Bereder, J.M., Porcheron, J., Gomez-Portilla, A., Shen, P., Deraco, M., Rat, P., 2004. Cytoreductive surgery combined with perioperative intraperitoneal chemotherapy for the management of peritoneal carcinomatosis from colorectal cancer: a multi-institutional study. J. Clin. Oncol. 22 (16), 3284–3292.

Griffin, D.R., Weaver, W.M., Scumpia, P.O., Di Carlo, D., Segura, T., 2015. Accelerated wound healing by injectable microporous gel scaffolds assembled from annealed building blocks. Nat. Mater. 14, 737–744.

Group, G.M.-a.T.G., 2002. Chemotherapy in adult high-grade glioma: a systematic review and meta-analysis of individual patient data from 12 randomised trials. The Lancet 359, 1011-1018.

Hasovits, C., Clarke, S., 2012. Pharmacokinetics and pharmacodynamics of intraperitoneal cancer chemotherapeutics. Clin. Pharmacokinet. 51 (4), 203–224.

Huo, S., Ma, H., Huang, K., Liu, J., Wei, T., Jin, S., Zhang, J., He, S., Liang, X.-J., 2013. Superior penetration and retention behavior of 50 nm gold nanoparticles in tumors. Cancer Res. 73 (1), 319–330.

Jain, E., Hill, L., Canning, E., Sell, S.A., Zustiak, S.P., 2017. Control of gelation, degradation and physical properties of polyethylene glycol hydrogels through the chemical and physical identity of the crosslinker. J. Mater. Chem. B 5 (14), 2679–2691.

Jansen, L.E., Negrón-Piñeiro, L.J., Galarza, S., Peyton, S.R., 2018. Control of thiol-maleimide reaction kinetics in PEG hydrogel networks. Acta Biomater. 70, 120–128.

Kohane, D.S., Langer, R., 2010. Biocompatibility and drug delivery systems. Chem. Sci. 1 (4), 441–446.

Kohane, D.S., Tse, J.Y., Yeo, Y., Padera, R., Shubina, M., Langer, R., 2006. Biodegradable polymeric microspheres and nanospheres for drug delivery in the peritoneum. Journal of Biomedical Materials Research Part A: An Official Journal of The Society for Biomaterials, The Japanese Society for Biomaterials, and The Australian Society for Biomaterials and the Korean Society for Biomaterials 77A (2), 351–361.

Kroger, S.M., Hill, L., Jain, E., Stock, A., Bracher, P.J., He, F., Zustiak, S.P., 2020. Design of Hydrolytically Degradable Polyethylene Glycol Crosslinkers for Facile Control of Hydrogel Degradation. Macromol. Biosci. 20 (10), 2000085.

Lee, S., Tong, X., Yang, F., 2016. Effects of the poly (ethylene glycol) hydrogel crosslinking mechanism on protein release. Biomater. Sci. 4 (3), 405–411.

Li, L., Wang, N., Jin, X., Deng, R., Nie, S., Sun, Lu., Wu, Q., Wei, Y., Gong, C., 2014. Biodegradable and injectable in situ cross-linking chitosan-hyaluronic acid based hydrogels for postoperative adhesion prevention. Biomaterials 35 (12), 3903–3917.

Li, Y., Rodrigues, J., Tomás, H., 2012. Injectable and biodegradable hydrogels: gelation, biodegradation and biomedical applications. Chem. Soc. Rev. 41 (6), 2193–2221.

Mirahmadi, N., Babaei, M.H., Vali, A.M., Dadashzadeh, S., 2010. Effect of liposome size on peritoneal retention and organ distribution after intraperitoneal injection in mice. Int. J. Pharm. 383 (1-2), 7–13.

Ngo, W., Ahmed, S., Blackadar, C., Bussin, B., Ji, Q., Mladjenovic, S.M., Sepahi, Z., Chan, W.C.W., 2022. Why nanoparticles prefer liver macrophage cell uptake in vivo. Adv. Drug Deliv. Rev. 185, 114238. https://doi.org/10.1016/j.addr.2022.114238.

Nguyen, M.K., Lee, D.S., 2010. Injectable biodegradable hydrogels. Macromol. Biosci. 10 (6), 563–579.

Nie, T., Baldwin, A., Yamaguchi, N., Kiick, K.L., 2007. Production of heparin-functionalized hydrogels for the development of responsive and controlled growth factor delivery systems. J. Control. Release 122 (3), 287–296.

Oyarzun-Ampuero, F.A., Rivera-Rodríguez, G.R., Alonso, M.J., Torres, D., 2013. Hyaluronan nanocapsules as a new vehicle for intracellular drug delivery. Eur. J. Pharm. Sci. 49 (4), 483–490.

Parayath, N.N., Parikh, A., Amiji, M.M., 2018. Repolarization of tumor-associated macrophages in a genetically engineered nonsmall cell lung cancer model by intraperitoneal administration of hyaluronic acid-based nanoparticles encapsulating microRNA-125b. Nano Lett. 18 (6), 3571–3579.

Pereira, R.F., Bártolo, P.J., 2014. Photopolymerizable hydrogels in regenerative medicine and drug delivery. Future Medicine.

Phelps, E.A., Enemchukwu, N.O., Fiore, V.F., Sy, J.C., Murthy, N., Sulchek, T.A., Barker, T.H., García, A.J., 2012. Maleimide Cross-Linked Bioactive PEG Hydrogel Exhibits Improved Reaction Kinetics and Cross-Linking for Cell Encapsulation and In Situ Delivery. Adv. Mater. 24 (1), 64–70.

Phelps, E.A., Templeman, K.L., Thulé, P.M., García, A.J., 2015. Engineered VEGF-releasing PEG–MAL hydrogel for pancreatic islet vascularization. Drug delivery and translational research 5 (2), 125–136.

Sadzuka, Y., Hirota, S., Sonobe, T., 2000. Intraperitoneal administration of doxorubicin encapsulating liposomes against peritoneal dissemination. Toxicol. Lett. 116 (1-2), 51–59.

Schädlich, A., Rose, C., Kuntsche, J., Caysa, H., Mueller, T., Göpferich, A., Mäder, K., 2011. How stealthy are PEG-PLA nanoparticles? An NIR in vivo study combined with detailed size measurements. Pharm. Res. 28 (8), 1995–2007.

Schoenmakers, R.G., van de Wetering, P., Elbert, D.L., Hubbell, J.A., 2004. The effect of the linker on the hydrolysis rate of drug-linked ester bonds. J. Control. Release 95 (2), 291–300.

Senger, D.R., Galli, S.J., Dvorak, A.M., Perruzzi, C.A., Harvey, V.S., Dvorak, H.F., 1983. Tumor cells secrete a vascular permeability factor that promotes accumulation of ascites fluid. Science 219 (4587), 983–985.

Shimada, T., Nomura, M., Yokogawa, K., Endo, Y., Sasaki, T., Miyamoto, K.-I., Yonemura, Y., 2005. Pharmacokinetic advantage of intraperitoneal injection of docetaxel in the treatment for peritoneal dissemination of cancer in mice. J. Pharm. Pharmacol. 57 (2), 177–181.

Siegel, R., Jemal, A., 2015. Cancer facts & figures 2015. American Cancer Society Cancer Facts & Figures.

Siegel, R., Ma, J., Zou, Z., Jemal, A., 2014. Cancer statistics, 2014: Cancer Statistics, 2014. CA Cancer J. Clin. 64 (1), 9–29.

Simón-Gracia, L., Hunt, H., Scodeller, P.D., Gaitzsch, J., Braun, G.B., Willmore, A.-M., Ruoslahti, E., Battaglia, G., Teesalu, T., 2016. Paclitaxel-loaded polymersomes for enhanced intraperitoneal chemotherapy. Mol. Cancer Ther. 15 (4), 670–679.

Štaka, I., Cadete, A., Surikutchi, B.T., Abuzaid, H., Bradshaw, T.D., Alonso, M.J., Marlow, M., 2019. A novel low molecular weight nanocomposite hydrogel formulation for intra-tumoural delivery of anti-cancer drugs. Int. J. Pharm. 565, 151–161.

Storozhylova, N., 2018. title., Nantes.

Storozhylova, N., Crecente-Campo, J., Cabaleiro, D., Lugo, L., Dussouy, C., Simões, S., Monteiro, M., Grandjean, C., Alonso, M.J., 2020. An In Situ Hyaluronic Acid-Fibrin Hydrogel Containing Drug-Loaded Nanocapsules for Intra-Articular Treatment of Inflammatory Joint Diseases. Regener. Eng. Transl. Med. 6 (2), 201–216.

Sugarbaker, P.H., 1998. Intraperitoneal chemotherapy and cytoreductive surgery for the prevention and treatment of peritoneal carcinomatosis and sarcomatosis, Seminars in surgical oncology. Wiley Online Library 14 (3), 254–261.

Tsai, M., Lu, Z.e., Wang, J., Yeh, T.-K., Wientjes, M.G., Au, J.-S., 2007. Effects of carrier on disposition and antitumor activity of intraperitoneal Paclitaxel. Pharm. Res. 24 (9), 1691–1701.

Van der Speeten, K., Stuart, O.A., Sugarbaker, P.H., 2009. Pharmacokinetics and pharmacodynamics of perioperative cancer chemotherapy in peritoneal surface malignancy. The Cancer Journal 15, 216–224.

Vintiloiu, A., Leroux, J.-C., 2008. Organogels and their use in drug delivery—a review. J. Control. Release 125 (3), 179–192.

Walker, J.L., Armstrong, D.K., Huang, H.Q., Fowler, J., Webster, K., Burger, R.A., Clarke-Pearson, D., 2006. Intraperitoneal catheter outcomes in a phase III trial of intravenous versus intraperitoneal chemotherapy in optimal stage III ovarian and primary peritoneal cancer: a Gynecologic Oncology Group Study. Gynecol. Oncol. 100 (1), 27–32.

Wang, Y., Gong, C., Yang, L., Wu, Q., Shi, S., Shi, H., Qian, Z., Wei, Y., 2010. 5-FU-hydrogel inhibits colorectal peritoneal carcinomatosis and tumor growth in mice. BMC cancer 10, 402.

Xu, L., Yu, H., Yin, S., Zhang, R., Zhou, Y., Li, J., 2015. Liposome-based delivery systems for ginsenoside Rh2: in vitro and in vivo comparisons. J. Nanopart. Res. 17, 415.

Xu, S., Fan, H., Yin, Li., Zhang, J., Dong, A., Deng, L., Tang, H., 2016. Thermosensitive hydrogel system assembled by PTX-loaded copolymer nanoparticles for sustained intraperitoneal chemotherapy of peritoneal carcinomatosis. Eur. J. Pharm. Biopharm. 104, 251–259.

Yang, K., Gong, H., Shi, X., Wan, J., Zhang, Y., Liu, Z., 2013. In vivo biodistribution and toxicology of functionalized nano-graphene oxide in mice after oral and intraperitoneal administration. Biomaterials 34, 2787–2795.

Yeo, Y., Ito, T., Bellas, E., Highley, C.B., Marini, R., Kohane, D.S., 2007. In situ cross-linkable hyaluronan hydrogels containing polymeric nanoparticles for preventing postsurgical adhesions. Ann. Surg. 245 (5), 819–824.

Yonemura, Y., Endou, Y., Bando, E., Kuno, K., Kawamura, T., Kimura, M., Shimada, T., Miyamoto, K.-I., Sasaki, T., Sugarbaker, P.H., 2004. Effect of intraperitoneal administration of docetaxel on peritoneal dissemination of gastric cancer. Cancer Lett. 210 (2), 189–196.

Yu, J., Xu, X.u., Yao, FuLin, Luo, Z., Jin, L., Xie, BinBin, Shi, S., Ma, H., Li, XingYi, Chen, H., 2014. In situ covalently cross-linked PEG hydrogel for ocular drug delivery applications. Int. J. Pharm. 470 (1-2), 151–157.

Zustiak, S.P., Leach, J.B., 2010. Hydrolytically degradable poly (ethylene glycol) hydrogel scaffolds with tunable degradation and mechanical properties. Biomacromolecules 11 (5), 1348–1357.

Zustiak, S.P., Leach, J.B., 2011. Characterization of protein release from hydrolytically degradable poly (ethylene glycol) hydrogels. Biotechnol. Bioeng. 108 (1), 197–206.